POPULATION DYNAMICS

Interactions between demography and environmental effects are important determinants of population dynamics

Marlène Gamelon,[1]* Vidar Grøtan,[1] Anna L. K. Nilsson,[2] Steinar Engen,[3] James W. Hurrell,[4] Kurt Jerstad,[5] Adam S. Phillips,[4] Ole W. Røstad,[6] Tore Slagsvold,[2] Bjørn Walseng,[7] Nils C. Stenseth,[2]* Bernt-Erik Sæther[1]*

Climate change will affect the population dynamics of many species, yet the consequences for the long-term persistence of populations are poorly understood. A major reason for this is that density-dependent feedback effects caused by fluctuations in population size are considered independent of stochastic variation in the environment. We show that an interplay between winter temperature and population density can influence the persistence of a small passerine population under global warming. Although warmer winters favor an increased mean population size, density-dependent feedback can cause the local population to be less buffered against occasional poor environmental conditions (cold winters). This shows that it is essential to go beyond the population size and explore climate effects on the full dynamics to elaborate targeted management actions.

INTRODUCTION

Understanding how to predict the future dynamics of natural populations as a response to global climatic change has become urgently required of ecologists and is crucial for producing appropriate management and conservation strategies. However, until now, this task has remained a challenge due to its scope because climate effects can influence the number of births, deaths, and immigrants in a population. Thus, climate effects have to be considered on all vital rates at all the (st)ages of the life cycle (*1*, *2*), which requires long-term detailed individual-based data. Otherwise, predictions regarding future dynamics may be severely biased (*3*). Moreover, climate may interact with density-dependent factors to affect the population dynamics (*4*–*6*). For example, when weather conditions affect limiting resources, climate effects should be studied in combination with density effects (*7*). Such interactions between climate and density may be complex (*1*, *8*–*11*), and although often ignored, this interactive effect may strongly affect the population dynamics (*9*, *10*). Consequently, reliable models of population dynamics in a changing environment must include such interactions between internal processes mainly operating through negative feedback of the number of individuals on the population growth rate and stochastic variation in the environment.

The white-throated dipper (*Cinclus cinclus*) is a small passerine bird widely distributed at northern latitudes that depends on open water for foraging and running water for nesting. The amount of ice during the winter influences the availability of feeding and breeding habitats (*12*). Previous studies on a population located in southern Norway have highlighted that the growth rate of that population was dependent on both environmental stochastic and deterministic density-dependent factors and that global warming should lead to an increase in the mean population size (*12*, *13*). However, none of these studies have yet explored the underlying demographic responses to changes in climate. Here, we develop an integrative framework of climate effects on population dynamics, including the interaction between density-dependent and environmental stochastic factors, as well as environmentally driven

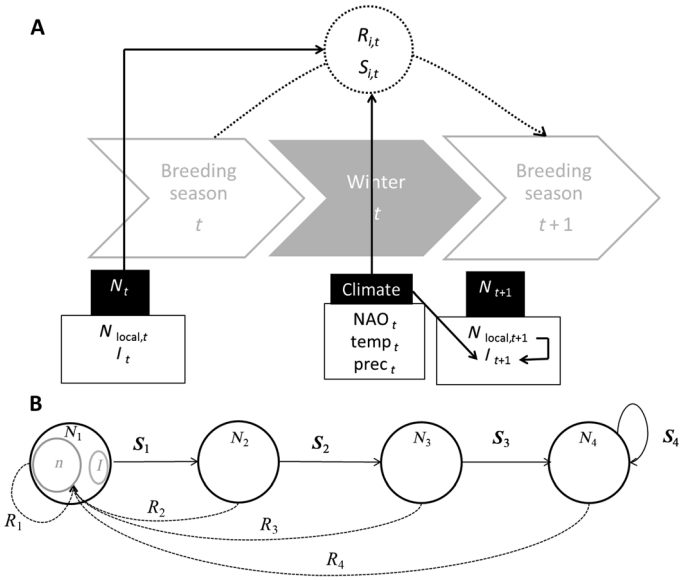

Fig. 1. CDDPM for the white-throated dipper population. (**A**) Recruitment rates $R_{i,t}$ and survival rates $S_{i,t}$ of age class i at year t may be influenced by density (N_t) [that is, sum of local ($N_{local,t}$) and immigrant breeding females (I_t)] and by winter conditions (that is, NAO_t, mean winter temperature $temp_t$, and mean winter precipitation $prec_t$). I_{t+1} may be influenced by $N_{local,t+1}$ and by winter conditions. (**B**) Solid lines correspond to survival transitions S_i from one age class N_i to the other, and dotted lines correspond to recruitment rates R_i. Note that age class 1 corresponds to the sum of daughters locally recruited n and newly immigrant breeding females I and that local breeding females N_{local} include all females in the population except the new immigrants (that is, $N_{local} = n + N_2 + N_3 + N_4$).

[1]Centre for Biodiversity Dynamics, Department of Biology, Norwegian University of Science and Technology, 7491 Trondheim, Norway. [2]Centre for Ecological and Evolutionary Synthesis, Department of Biosciences, University of Oslo, 0316 Oslo, Norway. [3]Centre for Biodiversity Dynamics, Department of Mathematical Sciences, Norwegian University of Science and Technology, 7491 Trondheim, Norway. [4]National Center for Atmospheric Research, Boulder, CO 80307, USA. [5]Jerstad Viltforvaltning, Aurebekksveien 61, 4516 Mandal, Norway. [6]Department of Ecology and Natural Resource Management, Norwegian University of Life Sciences, 1432 Ås, Norway. [7]Norwegian Institute for Nature Research, Gaustadalléen 21, 0349 Oslo, Norway.
*Corresponding author. Email: marlene.gamelon@ntnu.no (M.G.); n.c.stenseth@ibv.uio.no (N.C.S.); bernt-erik.sather@ntnu.no (B.-E.S.)

immigration, survival, and fecundity. From this framework, we will predict the future persistence of the population using local climate scenarios.

RESULTS

Analyzing how environmental stochasticity and deterministic factors caused by density dependence affect survival, fecundity, and immigration rates is the first step required before constructing a more complex population model. To do so, we used individual-based data collected between 1979 and 2013 and considered four age classes of breeding females. Age class 1 corresponded to the first year of breeding (second calendar year of life), age class 2 to the second year of breeding and third calendar year of life, age class 3 to the third year of breeding and fourth calendar year of life, and age class 4 to older breeding females. For each year t and for each age class i, we estimated the survival $S_{i,t}$ and recruitment $R_{i,t}$ rates (that is, the contribution of breeding females of age class i to recruitment into the age class 1 breeding class next year) (see Materials and Methods) (Fig. 1 and fig. S1). Then, we investigated the effect of several climate variables related to winter weather on these age-specific demographic rates (Fig. 1A), as well as on the annual number of immigrant breeding females joining the local population. We particularly considered the effects of the North Atlantic Oscillation (NAO) index (*14*, *15*), local mean winter temperature (temp), and local mean winter precipitation (prec). We also investigated an effect of the total number of breeding females in the population (hereafter, density N_t) on the age-specific demographic rates (see Fig. 1A for a schematic of the modeling).

Mean winter temperature was always the best environmental explanatory variable for all demographic rates (table S1). Warmer winters had a positive effect on survival and recruitment rates for all age classes, and this effect was age-specific (table S2). The effects of winter temperature on recruitment corresponded to the effects on the first-year survival because winter is a critical season for the survival of the white-throated dipper (*12*). Moreover, the significant interactions between winter temperatures and density (Fig. 2, A and B, tables S1 and S2, and fig. S2) indicated that climate variation mainly affects the demographic rates at high densities, suggesting an indirect effect of climate through resource limitation. There was a complex interaction between mean winter temperature and density of local females (Fig. 2C and tables S1 and S2) in explaining the number of immigrant females entering

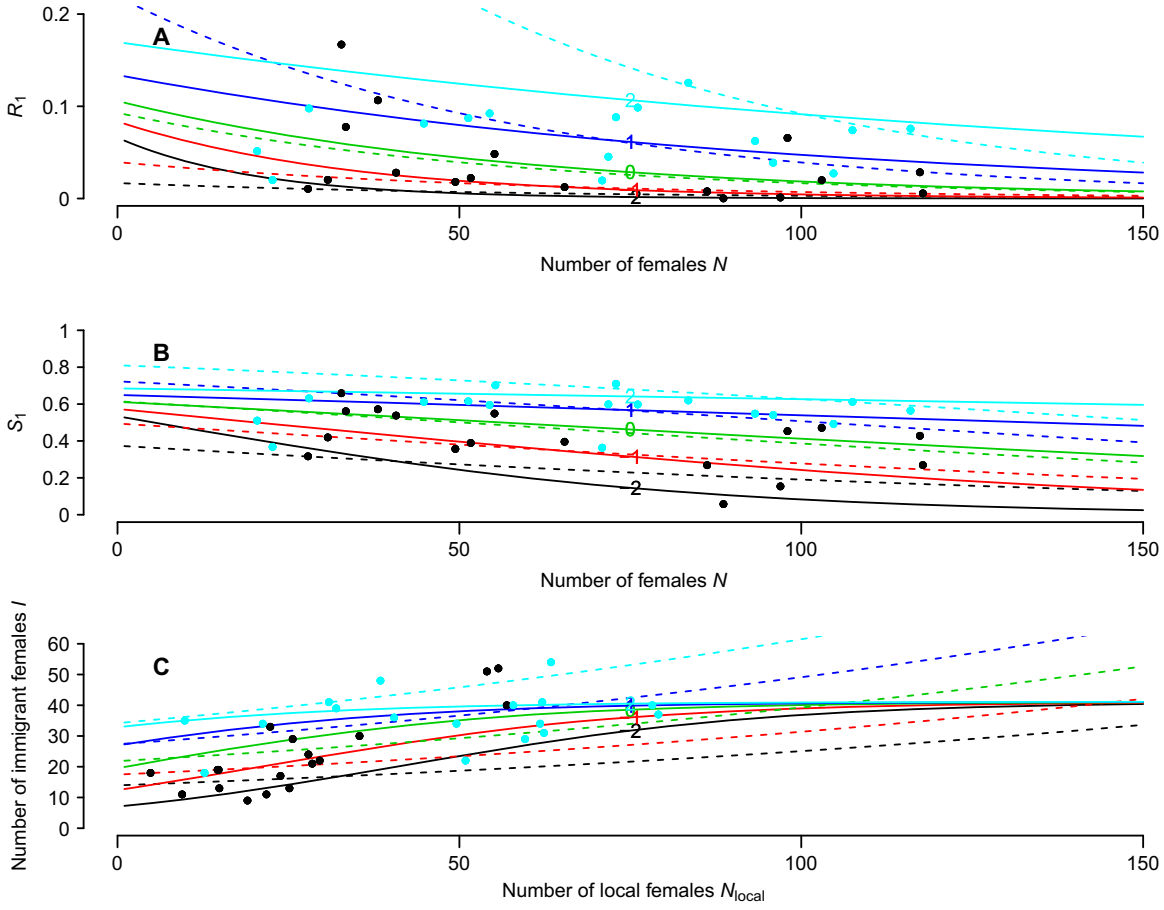

Fig. 2. Effect of density on demographic rates under different climate conditions from cold winters (standardized mean winter temperature, −2) to mild winters (standardized mean winter temperature, 2). (**A** and **B**) Relationships between demographic rates of age class 1 (recruitment R_1 and survival S_1) and density N (that is, total number of breeding females) for different winter conditions. (**C**) Relationship between the number of immigrant breeding females I and the total number of local breeding females N_{local} for different winter conditions. The solid lines have been drawn from the best models retained including density-dependent effects of winter conditions, whereas dotted lines have been drawn from models including density-independent effects of winter conditions (tables S1 and S2). Dots correspond to observations between 1979 and 2013 and, as an illustration, have been split into cold winters (black dots) versus mild winters (cyan dots).

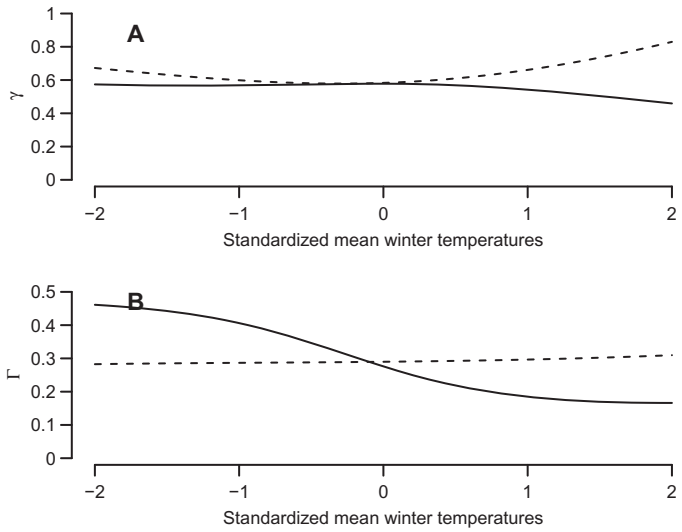

Fig. 3. Effect of a change in the number of females *N* or the mean winter temperatures temp on the population growth rate λ at equilibrium *K* under different climate conditions from cold winters (standardized mean winter temperature, −2) to mild winters (standardized mean winter temperature, 2). (**A**) $\gamma = -\left[\frac{\partial \log \lambda}{\partial \log N}\right]_K$ plotted against standardized mean winter temperatures and (**B**) $\Gamma = \left[\frac{\partial \log \lambda}{\partial \log \text{temp}}\right]_K$ plotted against standardized mean winter temperatures. Solid lines correspond to models including density-dependent effects of winter conditions, and dotted lines correspond to models including density-independent effects of winter conditions.

the local population (mainly females from age class 1; fig. S3). Particularly, milder winters were associated with higher number of immigrants than cold winters, but only when densities of local females were low (Fig. 2C). Mean winter temperature was consequently the main environmental factor affecting demographic rates, mostly likely operating indirectly through resource limitation.

Both population density and mean winter temperature in a given year thus affect survival, recruitment, and immigration rates (table S2), which in turn influence the age-specific densities in breeding females the following year and thus the total density (see Materials and Methods) (Fig. 1). The dynamical impact of variation in climate is therefore dependent on the population density. The strength of density dependence decreases slightly with increasing winter temperatures (Fig. 3A), and the effects of a change in temperature on the population growth rate are weaker in mild winters than in cold winters (Fig. 3B). As a consequence, under global warming, the probability of an increase in numbers at small population sizes (for example, $N = 20$) during a period of 40 years is much larger because of this interaction between density and temperature, compared to the case where density dependence and environmental stochasticity are considered as independent effects. Hence, predicted future population density becomes a complex function including the effects of environmental stochasticity and deterministic processes caused by density dependence, as well as their interaction.

To evaluate the power of the resulting climate-density–dependent population model (CDDPM) (Fig. 1) in predicting population size and structure, we started with the age-specific densities in 1979 and considered only the observed winter temperatures from 1979 to 2013 (fig. S4, left side). Then, we simulated 1000 stochastic trajectories in population sizes including demographic and environmental stochasticity (see Materials and Methods) from 1980 to 2013. Note that our population model can reconstruct the past fluctuations in population size very closely (fig. S5A) and past population structure as well (fig. S5, C and D), with a strong correlation r between observed and predicted number of breeding females in each group ($0.66 < r < 0.82$; see Materials and Methods).

Average surface temperatures at the closest model grid point (58.9°N, 7.5°E) were obtained from the Community Earth System Model (CESM) Large Ensemble Community Project (*16*) until 2050. These climate projections for the study area predict an increase in mean winter temperature in the coming years (fig. S4, right). We thus expect a future increase of survival and recruitment rates in all age classes (Fig. 2, A and B) and thus a growing mean population size. Further, warmer winters should not result in an increase in the number of immigrants. This is because the effect of increasing temperatures on the number of immigrants was shown to be strongly density-dependent, with the same number of immigrants whatever the winter temperature is when the local population was large (Fig. 2C). When including age-specific densities in 2013 in the CDDPM and the local climate projections by 2050 (fig. S4, right) (see Materials and Methods), we effectively found that the mean population size will have increased by 2050 (Fig. 4A). Such an increase is likely specifically due to a growing number of local females (Fig. 4B) because our CDDPM predicts a somewhat constant number of immigrants (Fig. 4C). Our results suggest that warmer winters may increase the demographic performance factors (that is, survival and recruitment) of the local population, which in turn reduces the proportion of immigrants joining the population through a density-dependent feedback on the number of immigrants. The expected changes in climate will reduce the rate of immigration into the population. This full understanding of the demographic mechanisms under climate change may not be achieved using a more typical population model including density-independent effects of climate. Because of the absence of interaction between winter conditions and density, such type of model overestimates the number of immigrants joining the local population at high densities during mild winters (Figs. 2C and 4C, dotted lines) and tends to underestimate survival and recruitment rates of local birds (Figs. 2, A and B, and 4B and fig. S2, dotted lines). Likewise, at mild winters, it overestimates the effect of a change in the number of females and the effect of a change in mean winter temperatures on the population growth rate at equilibrium K (Fig. 3, dotted lines). Therefore, although neglecting interaction between climate and density may provide a reliable measure of total population size under climate change (Fig. 4A), it does not allow for precise identification of the underlying processes.

DISCUSSION

Predictions of large declines and even extinctions caused by climate change of natural populations belonging to different taxa are growing in the literature (*17*). The present study shows that our white-throated dipper population located at the northern latitude may benefit from global warming in terms of abundance (Fig. 4A). Going beyond the total population abundance, we have reconstructed the full dynamics of the population and disentangled the demographic responses of the population to environmental variations. Our results suggest that the expected increase of density may have important consequences to the way our population will respond to future environmental changes because of dynamical transitions caused by an interaction between density dependence and environmental stochasticity (Figs. 2 and 3).

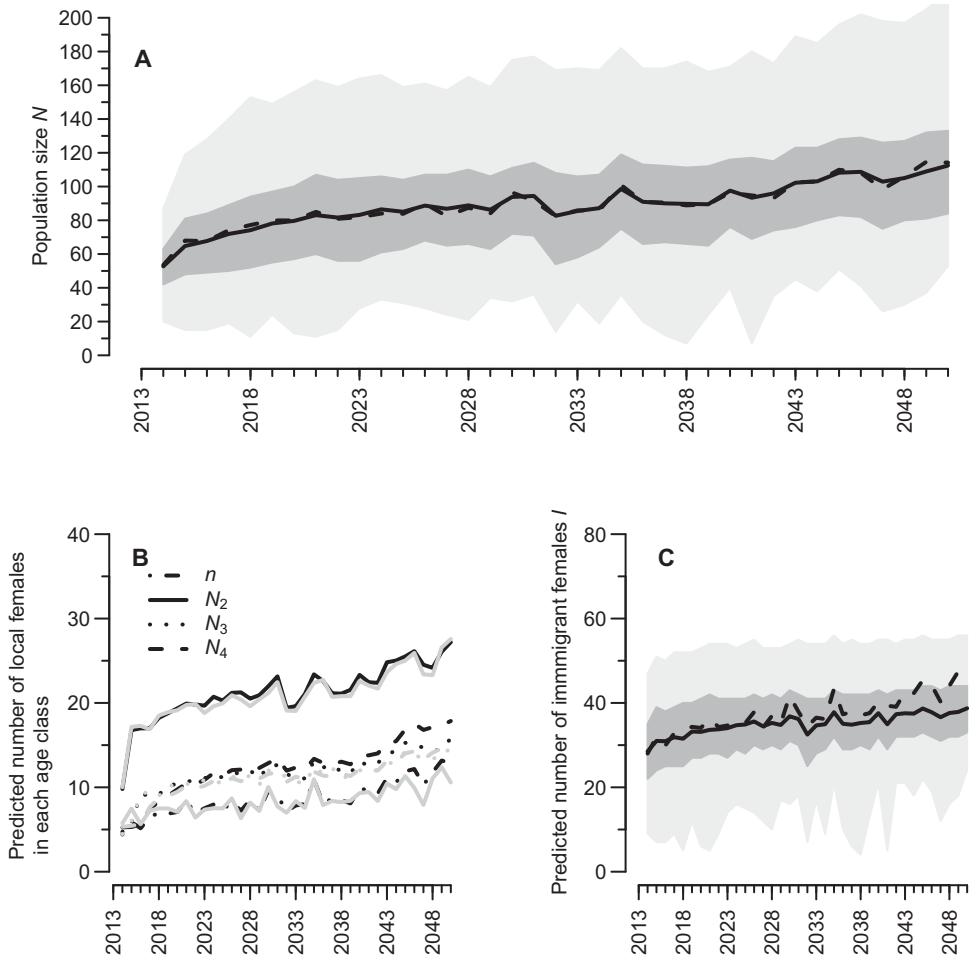

Fig. 4. Predicted densities between 2014 and 2050. (**A**) Total number of breeding females in the population in the future consists of (**B**) breeding females locally recruited (*n*), of age classes 2 (N_2), 3 (N_3), and 4 and older (N_4), and (**C**) newly arriving immigrant breeding females *I*. Predicted densities are provided by the CDDPM from climate scenarios available for the study site (fig. S4, right). Shaded dark gray corresponds to 50% and light gray corresponds to 95% prediction intervals associated with the predicted densities. To improve the readability, confidence intervals are not shown for (B). Dotted lines on (A) and (C) as well as gray lines on (B) correspond to models including density-independent effects of winter conditions.

Whereas at low density, survival and recruitment rates only slightly depend on winter temperatures (Fig. 2, A and B, and fig. S2), at high density, they become strongly dependent on winter conditions and are less buffered against poor environmental conditions (cold winters) (Fig. 2, A and B, and fig. S2). These findings highlight that, in addition to reduced immigration rate (Figs. 2C and 4C), the local population will likely be less buffered against occasional cold winters in the coming years. Our findings highlight that predicting the putative effects of global warming on natural populations requires a detailed picture of the dynamics of the populations. This integrative predictive framework of climate effects on population dynamics can help to elaborate targeted management actions on specific demographic rates of any population for which long-term individual-based data and climate scenarios are available.

MATERIALS AND METHODS

General approach

Our aim was to build a population model that includes climate effects on all demographic rates and at all ages of the life cycle of a white-throated dipper population while also accounting for other sources of environmental and demographic stochasticity and, in addition, density dependence. The model was built to, first, gain a good understanding of the demographic responses of the population to changes in its environment and, second, use this knowledge to project the fate of the population under different climate scenarios. We proceeded by several steps:

(i) We estimated the annual survival and recruitment rates of breeding females of age classes 1, 2, 3, and 4. We also jointly estimated the annual age-specific densities. These estimates were obtained from 1978 to 2013.

(ii) We explored the effects of climate variables (mean winter temperature, mean winter precipitation, and NAO index) and density on age-specific survival and recruitment rates and also on the number of immigrants joining the population.

(iii) On the basis of these relationships between demographic rates and climate-density, we built a CDDPM that predicts the age-specific numbers of breeding females under given conditions of climate-density. Using the observed time series of climate variables between 1979 and 2013, we reconstructed the past population structure and compared it with the observed number of breeding females during this period.

(iv) By feeding this CDDPM with climate scenarios from the study area, we projected the population to mid-century and examined its properties (population structure and population size).

White-throated dipper data

The studied population is located in the river system of Lyngdalselva in southern Norway (58°08′–58°40′N, 6°56′–7°20′E). The study site covers 60 km inland from the river mouth, and the river is interrupted by Lake Lygne. The white-throated dipper (*C. cinclus*) is a 50- to 70-g small passerine bird species distributed in mountainous regions across the Palearctic. It is a short-lived species; the oldest breeding female recorded in our population was 8 years of age. This species depends on open water for foraging and running water for nesting. The amount of ice during the winter thus influences the availability of feeding and breeding habitats. Breeding sites are concentrated on the many small tributaries and on rapids in the main river. Locations of breeding territories span from sea level to an altitude of about 600 m above sea level.

From 1978 to 2013, all breeding sites were visited during the nest building period to identify breeding pairs and record occupied nests, denoted as C_t. During visits in the breeding season, fledglings were ringed, ringed mothers were identified, and unringed mothers were given a ring to allow for future identifications. These unringed mothers (1094 over the study period, with 233 of them females of unknown age) were assumed to have immigrated into the population during the year in question. The following year, they are then considered to be local females. The mother was not identified in 88 of the occupied nests. Overall, 992 breeding females of known age (local and immigrant) were monitored, providing capture-recapture (CR) data of known age females. Moreover, ringed fledglings were recorded as recruited to the breeding population if they were caught breeding in a subsequent year. From the monitoring of breeding females of known age, we reported for each year t the observed number of breeding females in age class i ($B_{i,t}$) and also the observed number of locally recruited females produced per age class i ($J_{i,t}$). In total, this type of demographic data based on reproductive success consisted of 1880 breeding events. One hundred fourteen females were locally recruited.

Estimating annual age-specific demographic rates and densities using an IPM

We simultaneously integrated the recorded number of occupied nests (C_t), CR data of females with known age, and data on reproductive success (that is, $B_{i,t}$ and $J_{i,t}$) into a Bayesian integrated population model (IPM) (*18*). This allows estimating annual survival, recruitment, and densities (that is, the number of breeding females N) for each age class. Note that we defined density here as the annual number of breeding females because of the complexity of the breeding system in this species (*13*). Females become reproductively mature in their first spring, which is the second calendar year of life. We used four age classes of breeding females, with age class 1 corresponding to the first year of breeding (second calendar year of life), age class 2 to the second year of breeding and third calendar year of life, age class 3 to the third year of breeding and fourth calendar year of life, and age class 4 to older breeding females. The joint analysis of these three data sets (recorded number of occupied nests, CR data, and data on reproductive success) increases the precision of the estimates of the shared parameters. Such a framework allows accounting for observation error associated with the recorded number of nests (*19*), for the incomplete information on age structure in the monitoring data (for example, some females are of unknown age), for imperfect detection (for example, recapture probability is not 1), for emigration in the first year of life, which is potentially high in this species (*20*), and for demographic stochasticity (*21*).

The model was fitted within the Bayesian framework, and noninformative priors were specified for all the parameters, allowing the inference to be dominated by information in the data and not by the information in the priors. Markov chain Monte Carlo (MCMC) simulation was used for parameter estimation. To assess convergence, we ran four independent chains with different starting values for 1,000,000 MCMC iterations, with a burn-in of 500,000 iterations, thinning every 1000th observation and resulting in 2000 posterior samples. We used the Brooks and Gelman diagnostic $\hat{R}$ to assess the convergence of the simulations and used the rule $\hat{R} < 1.02$ to determine whether convergence was reached (*22*). The analyses were implemented using JAGS version 3.4.0 (*23*) called from R version 3.1.1 (*24*) with package R2jags (*25*). For a full description of the IPM, the priors used, and the R code to fit the IPM, see the example on great tit *Parus major* (*26*).

The IPM allowed us to estimate for each year t the posterior means and the 95% credible intervals (CRIs) of the apparent survival rates $S_{i,t}$ between age class i and $i + 1$ and the recruitment rates $R_{i,t}$ (that is, the contribution of breeding females of age class i to recruitment into the age class 1 breeding class next year) (fig. S1). We also estimated for each year t the number of local ($N_{\text{local},t}$) and immigrant (I_t) breeding females in each age class $N_{i,t}$ and in total N_t (fig. S3). To ensure that the priors for initial population sizes did not influence estimates of demographic rates and density in each age class during the first year of the study (that is, in 1978), we considered estimates provided by our IPM from 1979 onward.

Climate data

Both global and local weather conditions during the winter months have been shown to influence the growth rate of this population (*12*, *13*). As a measure of global winter conditions, we used the extended winter NAO index (December to March). This index is a commonly used weather variable influencing numerous winter climatic variables in the Northern Hemisphere (*14*, *27*). The NAO index was provided by the Climate and Global Dynamics Division, National Center for Atmospheric Research, Boulder, CO (https://climatedataguide.ucar.edu/) (*14*). We used the mean winter temperature (temp) and mean winter precipitation (prec) (December to February) of the whole region called Sørlandet as measures of local weather conditions. These data were available from the Norwegian Meteorological Institute (www.yr.no/sted/Norge/Vest-Agder/Audnedal/Konsmo~6051/klima.vinter.html).

Effects of climate, density, and their interaction on demographic rates

The IPM was used to estimate age-specific demographic rates and age-specific densities (figs. S1 and S3). Once these were estimated, we investigated the combined effects of both deterministic and environmental stochastic factors on demographic rates of all ages. We linked annual age-specific demographic rates as response variables to annual densities N_t and winter conditions as explanatory variables. Because the considered environmental variables can strongly covary, we looked for possible multicollinearity among explanatory variables that can lead to high SEs and difficulties in interpreting parameter estimates in regressions (*28*). We thus calculated Spearman pairwise correlation coefficients ρ and used the rule $\rho < 0.5$ to determine whether two environmental variables could be included in the same model (*29*, *30*). Because all correlation coefficients ρ among weather variables were higher than 0.7, environmental variables were not included simultaneously in the tested models.

More specifically, survival between two successive breeding seasons t and $t+1$ could be affected by the number of breeding females at time t in the population and also by winter conditions between the two breeding seasons (that is, winter t) (Fig. 1A). Therefore, we linked the age-specific survival rates $S_{i,t}$ (on a logit scale) to density at t N_t and to environmental conditions during winter at t. Because the effect of density and climate may be age-specific, we explored the interaction between age and environmental conditions and also the interaction between age and density. To account for the nonindependence of the survival rates among age classes of a given year, we included the year as a random effect. As a consequence, the global linear-mixed model (LMM) investigating an effect of deterministic and environmental stochastic factors on survival rates of age class i took the following form

$$\text{logit}(S_{i,t}) = \mu + \beta_{1,i}\, a + \beta_2\, E_t + \beta_3\, N_t + \beta_{4,i}[\, a \times E_t] + \beta_{5,i}[a \times N_t] + \beta_{\text{year}}\, \text{year} + \varepsilon_{S_{i,t}} \quad (1)$$

where μ is the intercept, a is the age class (that is, 1, 2, 3, and 4), E_t is one environmental variable (that is, NAO index, temp, or prec), N_t is the density, β are the regression coefficients, year is the random effect, and $\varepsilon_{S_{i,t}}$ corresponds to the residuals of the LMM. The Akaike information criterion corrected for small sample size (AICc) was used for model selection (*31*). In addition, because the effects of density on demographic rates may differ according to climate conditions, we tested for the interaction between each environmental variable and density using the Ricker model

$$\text{logit}(S_{i,t}) = \mu + \beta_{1,i}\, a + \beta_2\, E_t + \beta_3\, N_t \times e^{-k_{\text{R},i} \times E_t} + \beta_{4,i}[\, a \times E_t] + \beta_{5,i}[a \times N_t \times e^{-k_{\text{R},i} \times E_t}] + \beta_{\text{year}}\, \text{year} + \varepsilon_{S_{i,t}} \quad (2)$$

and the Beverton-Holt model

$$\text{logit}(S_{i,t}) = \mu + \beta_{1,i}\, a + \beta_2\, E_t + \beta_3 \frac{N_t}{1 + k_{\text{BH},i} \times E_t} + \beta_{4,i}[\, a \times E_t] + \beta_{5,i}\left[a \times \frac{N_t}{1 + k_{\text{BH},i} \times E_t}\right] + \beta_{\text{year}}\, \text{year} + \varepsilon_{S_{i,t}} \quad (3)$$

where $k_{\text{R},i}$ and $k_{\text{BH},i}$ are two parameters to be estimated. Note that $k_{\text{R},i}$ can be equal for all age classes ($k_{\text{R},1} = k_{\text{R},2} = k_{\text{R},3} = k_{\text{R},4}$). Similarly, $k_{\text{BH},i}$ can be equal for all age classes ($k_{\text{BH},1} = k_{\text{BH},2} = k_{\text{BH},3} = k_{\text{BH},4}$). Alternatively, $k_{\text{R},i}$ and $k_{\text{BH},i}$ may be age-specific. We used an optimization function to find the values of k_{R} and k_{BH} providing the lowest AICc. Then, we used AICc for model selection (*31*).

Similarly, the recruitment rate of a given breeding season t could be affected by the number of breeding females at time t in the population. Moreover, environmental conditions in the winter following the breeding season (that is, winter t) could potentially affect survival in the first year of life of the young produced (Fig. 1A). Therefore, we linked the age-specific recruitment rates $R_{i,t}$ (on a log scale) to density at t N_t and to environmental conditions during winter at t. The global LMM took the following form

$$\log(R_{i,t}) = \nu + \beta_{1,i}'\, a + \beta_2' E_t + \beta_3' N_t + \beta_{4,i}'[\, a \times E_t] + \beta_{5,i}'[a \times N_t] + \beta_6'\, \text{year} + \varepsilon_{R_{i,t}} \quad (4)$$

where ν is the intercept, a is the age class (that is, 1, 2, 3, and 4), E_t is one environmental variable (that is, NAO index, temp, or prec), N_t is the density, β' are the regression coefficients, year is the random effect, and $\varepsilon_{R_{i,t}}$ corresponds to the residuals of the LMM. As for survival, we also tested the interactions between each environmental variable and density with the Ricker and the Beverton-Holt models and used AICc for model selection.

The number of immigrants joining the population during the breeding season $t+1$ may be influenced by the winter conditions just before the breeding season (that is, winter t). In addition, the number of local breeding females N_{local} may influence the number of immigrant breeding females arriving into the population I (Fig. 1A). Therefore, we linked the number of immigrant breeding females I_{t+1} to the number of local breeding females at $t+1$ $N_{\text{local},t+1}$ and to environmental conditions during winter at t using a generalized linear mixed model (GLMM) with Poisson distribution and the year as random effect

$$I_{t+1} = \eta + \beta_{I,1}\, E_t + \beta_{I,2}\, N_{\text{local},t+1} + \beta_{I,\text{year}}\, \text{year} + \varepsilon_{I_{t+1}} \quad (5)$$

where η is the intercept, β_I are the regression coefficients, and $\varepsilon_{I_{t+1}}$ corresponds to the residuals of the GLMM. AICc was used for model selection. In addition, we tested the interaction between each environmental variable and the number of local breeding females on the number of immigrants joining the local population using a generalized logistic function with Poisson distribution and the year as a random effect

$$I_{t+1} = \frac{U}{1 + (e^{q_0 + q_1 \times E_t}) \times e^{-B \times N_{\text{local},t+1}}} + \beta_{I,\text{year}}\, \text{year} + \varepsilon_{I_{t+1}} \quad (6)$$

where U (which corresponds to the upper asymptote), q_0, q_1, and B were estimated using an optimization function aimed at minimizing the AICc value. The model with the lowest AICc was retained as the best one.

Climate-density–dependent population model

Because all the best models explaining variation in demographic rates retained an effect of mean winter temperatures (table S1), we standardized the variable "mean winter temperature" for the study period (that is, from 1979 to 2013) with the mean and the variance of the mean winter temperatures observed between 1921 and 2015 (fig. S4, left). Such standardization was useful for further population projections (see Climate and population projections). Each demographic rate may thus be defined as a function of density and mean winter temperature (table S2). Therefore, for given winter conditions and densities, age-specific survival and recruitment rates and also the number of immigrants joining the local population may be simulated (hereafter denoted as $S_{\text{sim}\ i,t}$, $R_{\text{sim}\ i,t}$, and $I_{\text{sim},t+1}$). As a result, the number of breeding females in the population $N_{\text{sim},t}$ may be simulated. Note that the number of immigrants joining the local population at $t+1$ $I_{\text{sim},t+1}$ was simulated from the function defined in table S2 using a Poisson distribution.

In detail, the total number of breeding females in the population at time $t+1$ $N_{\text{sim},t+1}$ corresponded to the sum of breeding females in each age class i $N_{\text{sim}\ i,t+1}$ at time $t+1$ (Fig. 1B)

$$N_{\text{sim},t+1} = N_{\text{sim}\ 1,\ t+1} + N_{\text{sim}\ 2,\ t+1} + N_{\text{sim}\ 3,\ t+1} + N_{\text{sim}\ 4,\ t+1} \quad (7)$$

(i) Because most of the immigrant breeding females were females of age class 1 (on average, 82% during the study period and fluctuating between 58 and 100%; fig. S3), we assumed that $N_{\text{sim }1,t+1}$ (first term in Eq. 7) corresponded to the sum of the number of daughters that was locally recruited into the population $n_{\text{sim},t+1}$ (that is, produced by the breeding females of each age class) and also of the number of immigrants $I_{\text{sim},t+1}$ arriving into the population

$$N_{\text{sim }1,t+1} = n_{\text{sim},t+1} + I_{\text{sim},t+1} \quad (8)$$

$n_{\text{sim},t+1}$ was modeled using a Poisson distribution to include demographic stochasticity

$$n_{\text{sim},t+1} \sim \text{Poisson}(N_{\text{sim }1,t} \times R_{\text{sim }1,t}) + \text{Poisson}(N_{\text{sim }2,t} \times R_{\text{sim }2,t}) + \text{Poisson}(N_{\text{sim }3,t} \times R_{\text{sim }3,t}) + \text{Poisson}(N_{\text{sim }4,t} \times R_{\text{sim }4,t}) \quad (9)$$

(ii) $N_{\text{sim }2,t+1}$ (second term in Eq. 7) corresponded to the number of females of age class 1 that survived from time t to time $t + 1$ and was modeled using a binomial process to include demographic stochasticity

$$N_{\text{sim }2,t+1} \sim \text{Bin}(N_{\text{sim }1,t}, S_{\text{sim }1,t}) \quad (10)$$

(iii) Similarly, $N_{\text{sim }3,t+1}$ and $N_{\text{sim }4,t+1}$ (the third and fourth terms in Eq. 7, respectively) corresponded to the number of females in the previous age class that survived from time t to time $t + 1$

$$N_{\text{sim }3,t+1} \sim \text{Bin}(N_{\text{sim }2,t}, S_{\text{sim }2,t}) \quad (11)$$

$$N_{\text{sim }4,t+1} \sim \text{Bin}(N_{\text{sim }3,t}, S_{\text{sim }3,t}) + \text{Bin}(N_{\text{sim }4,t}, S_{\text{sim }4,t}) \quad (12)$$

Therefore, for given winter conditions and densities, $S_{\text{sim }i,t}$, $R_{\text{sim }i,t}$, and $I_{\text{sim},t+1}$ may be computed (from the relationships shown in table S2). To account for sources of environmental stochasticity due to processes other than covariates included in the model, a covariance matrix Σ of "random year effect + $\varepsilon_{S_{i,t}}$," "random year effect + $\varepsilon_{R_{i,t}}$," and "random year effect + $\varepsilon_{I_{t+1}}$" was estimated, and new residuals were generated from a multivariate normal distribution with a covariance matrix equal to Σ. Then, $N_{\text{sim }1,t+1}$, $N_{\text{sim }2,t+1}$, $N_{\text{sim }3,t+1}$, and $N_{\text{sim }4,t+1}$ that are functions of $S_{\text{sim }i,t}$, $R_{\text{sim }i,t}$ and $I_{\text{sim},t+1}$, may be computed (Eqs. 8 to 12), and finally, the density $N_{\text{sim},t+1}$ may be simulated (Eq. 7).

Strength of density dependence and climate

The strength of the density dependence γ corresponds to the negative elasticity of the population growth rate λ with respect to changes in the total number of breeding females N, evaluated at the carrying capacity K: $\gamma = -\left[\frac{\partial \log \lambda}{\partial \log N}\right]_K$. That is, γ provides a measure of the effect of a small change of density (that is, N) on the population growth rate λ at the equilibrium. From the deterministic version of our CDDPM, γ was calculated for different standardized mean winter temperatures, from −2 to 2.

Similarly, evaluating the effect of a small change in mean winter temperature temp on λ at equilibrium may be calculated as $\Gamma = \left[\frac{\partial \log \lambda}{\partial \log \text{temp}}\right]_K$. From the deterministic version of our CDDPM, Γ was calculated for different standardized mean winter temperatures, from −2 to 2.

Using the CDDPM to reconstruct past population structure

Using the age-specific densities in 1979 that were previously estimated with the IPM and the standardized mean winter temperatures from 1979 to 2013 (fig. S4, left), we simulated $S_{\text{sim }i}$, $R_{\text{sim }i}$, I_{sim}, $N_{\text{sim }i}$, and finally N_{sim} over the study period. We simulated 1000 stochastic trajectories of population sizes (fig. S5). On the basis of the data from 1979, the observed density N (fig. S5A, thin line) was within the 95% prediction interval in 94.1% of the cases, and within the 50% prediction interval in 61.8% of the cases, indicating a good match between observed and predicted total population size. Note that the observed densities were the densities obtained from the IPM (that is, corrected for observation error, the incomplete information on age structure in the monitoring data, and imperfect detection). To ensure that the CDDPM correctly modeled the full development of the population and not only the total population size, we computed the Pearson's product-moment correlations r and their associated 95% confidence intervals between the observed and predicted number of breeding females in each age class. That is, we compared the observed population structure (fig. S5, B and C, thin lines) with the population structure predicted with the CDDPM (fig. S5, C and D, thick lines). In practice, for each year between 1979 and 2013, we estimated the mean number of breeding females in each age class among the 1000 simulated stochastic trajectories and compared it with the observed number of breeding females [$r_{I,I\text{sim}} = 0.79(0.62; 0.89)$, $r_{n,n\text{sim}} = 0.66(0.42; 0.82)$, $r_{N2,N2\text{sim}} = 0.78(0.60; 0.89)$, $r_{N3,N3\text{sim}} = 0.82(0.66; 0.91)$, $r_{N4,N4\text{sim}} = 0.72(0.50; 0.85)$].

Climate and population projections

We obtained from the CESM Large Ensemble Community Project (*16*) the daily average surface temperatures at the closest model grid point (58.9°N, 7.5°E) for 40 ensemble members [see the work of Kay *et al.* (*16*) for a full description of the climate projections]. For these 40 ensemble members, we calculated the mean temperature for each winter (December to February) between 1921 and 2050. As with the observed temperatures (see Climate-density–dependent population model), we standardized the winter weather scenarios (with the mean and the variance of the mean winter temperatures predicted between 1921 and 2015). Thus, the mean and the SD used for standardizing each of the members were the mean of means and the mean of SDs calculated for each member. Such a rescaling allowed observed temperatures and climate scenarios (on average across all 40 of them) to be aligned between 1921 and 2015 so that they had the same mean and variance (fig. S4, right).

Using the age-specific densities in 2013 that were previously estimated with the IPM and these standardized values of mean winter temperatures, we simulated with the CDDPM 100 stochastic trajectories in population sizes per ensemble member from 2013 to 2050, resulting in a total of 4000 stochastic trajectories. We computed the 95 and 50% prediction intervals of the predicted total population size (Fig. 4A), of the number of local breeding females (Fig. 4B), and of the number of immigrant breeding females (Fig. 4C). All of these analyses were performed with R software (*24*).

SUPPLEMENTARY MATERIALS

Supplementary material for this article is available at http://advances.sciencemag.org/cgi/content/full/3/2/e1602298/DC1

fig. S1. Posterior means estimated from the IPM of the annual survival rates S_i and annual recruitment rates R_i (defined as the number of daughters locally recruited per breeding female) of breeding females of each age class *i* and their associated 95% CRI (gray lines) in the white-throated dipper population of Lyngdalselva, Norway, between 1979 and 2012.

fig. S2. Relationship between age-specific recruitment rates R_i or age-specific survival rates S_i and density *N* (that is, total number of breeding females) under different climate conditions from cold winters (standardized mean winter temperature, −2) to mild winters (standardized mean winter temperature, 2).

fig. S3. Posterior means estimated from the IPM of the number of local (in black) and immigrant (in gray) breeding females in each age class.

fig. S4. Standardized observed mean winter temperatures between 1979 and 2013 (corresponding to observed mean winter temperatures fluctuating between −7.3° and 1.6°C) and standardized predicted mean winter temperatures corresponding to 40 different climate scenarios between 2014 and 2050 in the study site.

fig. S5. Observed and predicted densities between 1979 and 2013.

table S1. Model selection for the effects of age class (*a*), density (*N*), mean winter temperatures (temp), mean winter precipitations (prec), and NAO index on age-specific recruitment rates $R_{i,t}$ (on a log scale) (that is, the number of daughters locally recruited per breeding female) and on age-specific survival rates $S_{i,t}$ (on a logit scale) of breeding females of age class *i* in Lyngdalselva, Norway, between 1979 and 2013.

table S2. Parameter estimates and their associated SE for the effects of age, density (*N*), standardized mean winter temperatures (temp), and their interaction on recruitment rates R_i (log-transformed) (that is, the number of daughters locally recruited per breeding female) and on survival S_i (logit-transformed) of breeding females of age class *i* in Lyngdalselva, Norway, between 1979 and 2013.

REFERENCES AND NOTES

1. T. Coulson, E. A. Catchpole, S. D. Albon, B. J. T. Morgan, J. M. Pemberton, T. H. Clutton-Brock, M. J. Crawley, B. T. Grenfell, Age, sex, density, winter weather, and population crashes in Soay sheep. *Science* **292**, 1528–1531 (2001).
2. S. Jenouvrier, Impacts of climate change on avian populations. *Glob. Chang. Biol.* **19**, 2036–2057 (2013).
3. V. Radchuk, C. Turlure, N. Schtickzelle, Each life stage matters: The importance of assessing the response to climate change over the complete life cycle in butterflies. *J. Anim. Ecol.* **82**, 275–285 (2013).
4. P. Turchin, Population regulation: Old arguments and a new synthesis, in *Population Dynamics: New Approaches and Synthesis*, N. Cappucino, P. W. Price, Eds. (Academic Press, 1995), pp. 19–40.
5. C. Barbraud, H. Weimerskirch, Climate and density shape population dynamics of a marine top predator. *Proc. Biol. Sci.* **270**, 2111–2116 (2003).
6. N. C. Stenseth, H. Viljugrein, T. Saitoh, T. F. Hansen, M. O. Kittilsen, E. Bølviken, F. Glöckner, Seasonality, density dependence, and population cycles in Hokkaido voles. *Proc. Natl. Acad. Sci. U.S.A.* **100**, 11478–11483 (2003).
7. M. Lima, M. A. Previtali, P. L. Meserve, Climate and small rodent dynamics in semiarid Chile: The role of lateral and vertical perturbations and intra-specific processes. *Clim. Res.* **30**, 125–132 (2006).
8. T. Royama, *Analytical Population Dynamics* (Springer Science & Business Media, 1992), 371 pp.
9. T. Coulson, T. H. Ezard, F. Pelletier, G. Tavecchia, N. C. Stenseth, D. Z. Childs, J. G. Pilkington, J. M. Pemberton, L. E. Kruuk, T. H. Clutton-Brock, M. J. Crawley, Estimating the functional form for the density dependence from life history data. *Ecology* **89**, 1661–1674 (2008).
10. N. C. Stenseth, K.-S. Chan, G. Tavecchia, T. Coulson, A. Mysterud, T. Clutton-Brock, B. Grenfell, Modelling non–Additive and nonlinear signals from climatic noise in ecological time series: Soay sheep as an example. *Proc. Biol. Sci.* **271**, 1985–1993 (2004).
11. M. S. Boyce, C. V. Haridas, C. T. Lee; The Nceas Stochastic Demography Working Group, Demography in an increasingly variable world. *Trends Ecol. Evol.* **21**, 141–148 (2006).
12. B.-E. Sæther, J. Tufto, S. Engen, K. Jerstad, O. W. Røstad, J. E. Skåtan, Population dynamical consequences of climate change for a small temperate songbird. *Science* **287**, 854–856 (2000).
13. A. L. K. Nilsson, E. Knudsen, K. Jerstad, O. W. Røstad, B. Walseng, T. Slagsvold, N. C. Stenseth, Climate effects on population fluctuations of the white-throated dipper *Cinclus cinclus*. *J. Anim. Ecol.* **80**, 235–243 (2011).
14. J. W. Hurrell, Decadal trends in the North Atlantic Oscillation: Regional temperatures and precipitation. *Science* **269**, 676–679 (1995).
15. N. C. Stenseth, G. Ottersen, J. W. Hurrell, A. Mysterud, M. Lima, K.-S. Chan, N. G. Yoccoz, B. Ådlandsvik, Review article. Studying climate effects on ecology through the use of climate indices: The North Atlantic Oscillation, El Niño Southern Oscillation and beyond. *Proc. Biol. Sci.* **270**, 2087–2096 (2003).
16. J. E. Kay, C. Deser, A. Phillips, A. Mai, C. Hannay, G. Strand, J. M. Arblaster, S. C. Bates, G. Danabasoglu, J. Edwards, M. Holland, P. Kushner, J.-F. Lamarque, D. Lawrence, K. Lindsay, A. Middleton, E. Munoz, R. Neale, K. Oleson, L. Polvani, M. Vertenstein, The Community Earth System Model (CESM) Large Ensemble project: A community resource for studying climate change in the presence of internal climate variability. *Bull. Am. Meteorol. Soc.* **96**, 1333–1349 (2015).
17. M. Z. Peery, R. J. Gutiérrez, R. Kirby, O. E. LeDee, W. LaHaye, Climate change and spotted owls: Potentially contrasting responses in the Southwestern United States. *Glob. Chang. Biol.* **18**, 865–880 (2012).
18. M. Schaub, F. Abadi, Integrated population models: A novel analysis framework for deeper insights into population dynamics. *J. Ornithol.* **152**, 227–237 (2011).
19. J.-D. Lebreton, O. Gimenez, Detecting and estimating density-dependence in wildlife populations. *J. Wildl. Manage.* **77**, 12–23 (2013).
20. S. J. Tyler, S. J. Ormerod, J. M. S. Lewis, The post-natal and breeding dispersal of Welsh Dippers *Cinclus cinclus*. *Bird Study* **37**, 18–22 (1990).
21. R. Lande, Incorporating stochasticity, in *Population Viability Analysis*, S. R. Beissinger, D. R. McCullough, Eds. (University of Chicago Press, 2002), pp. 18–40.
22. S. P. Brooks, A. Gelman, General methods for monitoring convergence of iterative simulations. *J. Comput. Graph. Stat.* **7**, 434–455 (1998).
23. M. Plummer, in *Proceedings of the 3rd International Workshop on Distributed Statistical Computing*, K. Hornik, F. Leisch, A. Zeileis, Eds. (Technische Universität Wien, 2003), pp. 20–22.
24. R Development Core Team, *R: A Language and Environment for Statistical Computing* (R Foundation for Statistical Computing, 2011).
25. Y.-S. Su, M. Yajima, *R2jags: A Package for Running Jags* (R. R package version 0.03-08, 2012).
26. M. Gamelon, V. Grøtan, S. Engen, E. Bjørkvoll, M. E. Visser, B. E. Saether, Density dependence in an age-structured population of great tits: Identifying the critical age classes. *Ecology* **97**, 2479–2490 (2016).
27. N. C. Stenseth, A. Mysterud, Weather packages: Finding the right scale and composition of climate in ecology. *J. Anim. Ecol.* **74**, 1195–1198 (2005).
28. M. H. Graham, Confronting multicollinearity in ecological multiple regression. *Ecology* **84**, 2809–2815 (2003).
29. B. Price, C. A. McAlpine, A. S. Kutt, S. R. Phinn, D. V. Pullar, J. A. Ludwig, Continuum or discrete patch landscape models for savanna birds? Towards a pluralistic approach. *Ecography* **32**, 745–756 (2009).
30. B. Price, A. S. Kutt, C. A. McAlpine, The importance of fine-scale savanna heterogeneity for reptiles and small mammals. *Biol. Conserv.* **143**, 2504–2513 (2010).
31. K. P. Burnham, D. R. Anderson, *Model Selection and Multimodel Inference: A Practical Information-Theoretic Approach* (Springer Science & Business Media, 2002), 488 pp.

Acknowledgments: We thank all the persons involved in the fieldwork and the CESM Large Ensemble Community Project and supercomputing resources provided by the National Science Foundation/Computational and Information Systems Laboratory/Yellowstone for the climate projection data. We thank S. C. Cunningham for correcting our English and two anonymous referees for their helpful comments on a previous draft. **Funding:** This work was partly supported by the Directorate for Nature Management (Norwegian Environment Agency), the European Research Council (grant STOCHPOP to B.-E.S.), and the Research Council of Norway through its Centres of Excellence funding scheme (project number 223257 to Centre for Biodiversity Dynamics and 179569 to Centre for Ecological and Evolutionary Synthesis). **Author contributions:** M.G., V.G., S.E., N.C.S., and B.-E.S. conceived the idea; J.W.H. and A.S.P. provided the climate projection data; K.J. and O.W.R. contributed to data collection; M.G. and V.G. analyzed the data; M.G. wrote the manuscript; and all authors contributed to revisions of the initial manuscript. **Competing interests:** The authors declare that they have no competing interests. **Data and materials availability:** All data needed to evaluate the conclusions in the paper are present in the paper and/or the Supplementary Materials. Additional data related to this paper may be requested from the authors.

Submitted 20 September 2016
Accepted 21 December 2016
Published 1 February 2017
10.1126/sciadv.1602298

Citation: M. Gamelon, V. Grøtan, A. L. K. Nilsson, S. Engen, J. W. Hurrell, K. Jerstad, A. S. Phillips, O. W. Røstad, T. Slagsvold, B. Walseng, N. C. Stenseth, B.-E. Sæther, Interactions between demography and environmental effects are important determinants of population dynamics. *Sci. Adv.* **3**, e1602298 (2017).

ScienceAdvances
AAAS

Interactions between demography and environmental effects are important determinants of population dynamics

Marlène Gamelon, Vidar Grøtan, Anna L. K. Nilsson, Steinar Engen, James W. Hurrell, Kurt Jerstad, Adam S. Phillips, Ole W. Røstad, Tore Slagsvold, Bjørn Walseng, Nils C. Stenseth and Bernt-Erik Sæther (February 1, 2017)

Sci Adv 2017, 3:.
doi: 10.1126/sciadv.1602298